Open Access

Functional Reconstruction of Structurally Complex Epitopes using CLIPS™ Technology#

P. Timmerman[1,2,*] W.C. Puijk[1], R.S. Boshuizen[1], P. van Dijken[1], J.W. Slootstra[1], F. J. Beurskens[3], P.W.H.I. Parren[3], A. Huber[4], M.F. Bachmann[4] and R.H. Meloen[1,5]

[1]*Pepscan Therapeutics BV, Zuidersluisweg 2, 8243 RC, Lelystad, The Netherlands*

[2]*Van 't Hoff Institute for Molecular Sciences, University of Amsterdam, The Netherlands*

[3]*Genmab, Yalelaan 60, 3584 CM Utrecht, The Netherlands*

[4]*Cytos Biotechnology AG, Schlieren, Switzerland*

[5]*Academic Biomedical Centre, University of Utrecht, The Netherlands*

Abstract: This review summarizes an illustrative set of data from our research on the reconstruction of structurally complex protein surfaces, i.e. those that fail to be mimicked properly by linear peptides. In the past 5 years, our newly developed **CLIPS™** technology has proven an extremely valuable tool for 1) binding site mapping of therapeutically relevant mAbs, 2) generating hyperimmune sera *via* immunization with **CLIPS** peptides, and 3) the generation of monoclonal antibodies (mAbs) *via* the use of hybridoma technology. We currently have data available for more than 50 therapeutic targets. The examples described in this review illustrate the potential of this powerful new technology.

Key Words: Peptide, protein mimicry, epitope, conformational, discontinuous, monoclonal antibodies, vaccine.

INTRODUCTION

The functional mimicry of a folded protein surface using peptides is a scientifically challenging problem. It has been commonly accepted that *"many proteins exert their biological activity through relatively small regions of their folded surfaces, so their actions could in principle be reproduced by much smaller "designer" molecules that retain these localized bioactive surfaces, but have improved pharmacodynamic and kinetic properties*" [1]. Peptide-based protein mimics have enormous value for the development of therapeutic antibodies or synthetic vaccines, where an increasing number of protein targets is being identified that is difficult to address by using standard techniques (HIV, GPCR's, etc.). Antibody-based immunotherapies are nowadays regarded as the most promising therapeutic approaches for life-threatening diseases, especially when combined with classical therapies [2, 3].

Occasionally, short linear peptides can mimic the function of a whole protein, but this approach is largely limited to unstructured N- and C-termini of proteins (Fig. **1**). In the early 1980s, Bittle and Dimarchi described the first example of (partial) protection of cattle for viral infection with foot-and-mouth-disease-virus (FMDV) *via* immunization with linear peptides derived from the coat-protein of the virus [4, 5]. Soon after, Langeveld *et al*. obtained complete protection of dogs against canine parvovirus (CPV) infection *via* immunization with linear peptides derived from the VP2-protein [6, 7]. Other studies showed that immunization with a 37-mer peptide derived from the C-terminus of human choriogonadotrophin (hCG; CTP37), the pregnancy hormone, renders women temporarily infertile [8, 9]. Following this observation, anti-hCG vaccination has been studied as means of affordable birth control in underdeveloped countries [9], and recently also as a potential therapy for the treatment of hCG-overexpressing tumors [10, 11].

For mimicry of conformational and/or discontinuous binding sites (Fig. **1B**) linear peptides generally fail, because they do not adopt the correct secondary and tertiairy structure. For that purpose, more elaborate tools are needed to position correctly the important functionalities in space, which is an absolute prerequisite for activity [12-14].

THERMODYNAMICS OF PROTEIN FOLDING AND THE PURPOSE OF SYNTHETIC SCAFFOLDS

In order to understand better why small peptides (20-30 amino acids) are not stably folded, contrary to the proteins they were derived of, it is important to consider why proteins unfold. Proteins exist in a dynamic equilibrium between a folded (F) and an unfolded state (U) (Fig. **2A**). The Gibbs free energy of folding is given by the following equation: $\Delta G_{F\text{-}U} = \Delta H_{F\text{-}U} - T\Delta S_{F\text{-}U}$. The folding process involves two opposing forces, i.e. the drive towards lower enthalpy ($\Delta H\downarrow$) and the drive towards maximum entropy ($\Delta S\uparrow$) [15]. The folded state is lowest in enthalpy. It is stabilized by

*Address correspondence to this author at Pepscan Therapeutics BV, Zuidersluisweg 2, 8243 RC Lelystad, The Netherlands; Tel: +31-320-225324; Fax: +31-320-225301; E-mail: p.timmerman@pepscan.com

#This review is partly based on a paper presented at the Vaccine Development Conference held at the University of Pittsburgh on 28-30 September 2008 (http://www.biacore.com/lifesciences/events/vaccine2008/home/index.html).

1875-0354/09

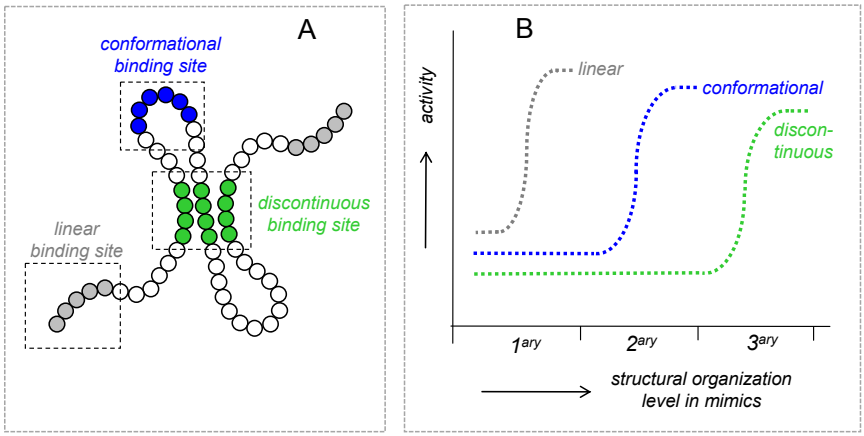

Fig. (1). Schematic representation of **A**) linear, conformational and discontinuous binding sites, and **B**) required level of structural organization in protein mimics for each of these.

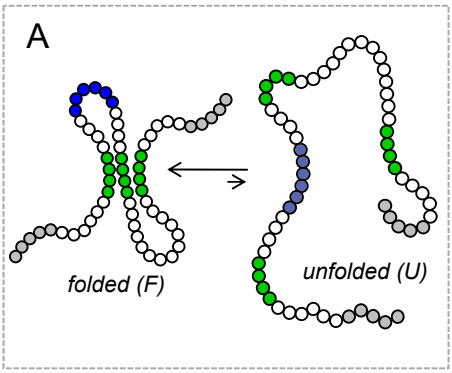

B

Energetic contribution	Energy (kcal/mol)
TΔS unfav (conform)	-350 to -1000
ΔH unfav (in F)	+200
ΔH fav (hydrophobic)	-275
ΔH fav (vanderWaals)	-225
ΔH fav (H-bond, electr)	-50 to -725
Overall: ΔG_{F-U}	**-5 to -10**

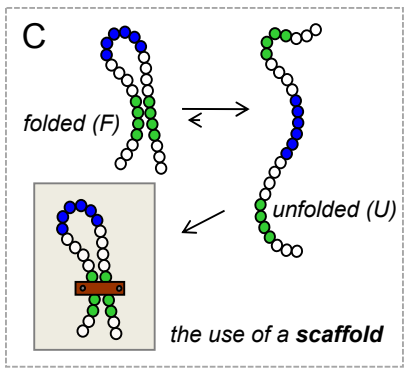

Fig. (2). Schematic illustration of **A**) dynamic equilibrium between folded and unfolded state of proteins, **B**) different enthalpic and entropic contribution to overall Gibbs free energy of folding, and **C**) unfolding of small peptides and stabilization of local protein structure by means of scaffold technology.

intramolecular interactions (hydrophobic, ionic, H-bond, etc.) between side and main chain elements. Hydrophobic parts stick together and form the inner core of the protein, while other groups remain at the outer, solvent-accessible surface. From an entropic point of view, the folded state is disfavored, since the protein likes to retain a maximal degree of conformational freedom. For structured proteins, the enthalpy term outweighs the entropy term (usually ~5-10 kcal/mol) and so the protein is stable in its folded state. However, this balance can be tipped over by heating, which explains why proteins denature at elevated temperatures (increasing importance of TΔS, ΔG_{F-U} becomes positive).

The majority of small peptides (20-30 amino acids) derived from intact proteins lack a well-defined structure in solution. In fact, removal of the remainder of the protein backbone has taken away the majority of stabilizing, enthalpic, interactions that normally give structure to the protein. The peptide requires an energetic compensation for this, to prevent it from remaining unstructured. Synthetic scaffolds can usually solve this problem by affixing the loose ends of the peptide. A scaffold is able to strongly reduce the unfavourable entropy term for spontaneous unfolding of the flexible peptide by lowering the number of possible conformations (Fig. **2C**). In this way, the scaffolded peptide may be able to adopt the same spatial structure as the corresponding sequence in the intact protein.

CLIPS™ TECHNOLOGY: MIMICRY OF CONFORMATIONAL AND DISCONTINUOUS EPITOPES

A variety of chemical methods is currently available for structural fixation of peptides into stable secondary structures, like α-helices [16-19], β-sheets [20], or β-hairpins [21-23], either *via* backbone or side chain functionalities (SS, Br-SH, CO_2H/NH_2, metathesis, CLICK chemistry) [19, 24, 25]. Some of these require special protection/deprotection protocols (CO_2H/NH_2) or the addition of a catalyst (SS, metathesis, CLICK), since otherwise the reaction rates are too slow (SS, CLICK). This may severely limit applicability to the purpose of binding site reconstruction.

We recently developed a novel and generic technology for structural fixation of linear peptides (Fig. **3**) [26]. This technology, termed **CLIPS™** technology (**C**hemical **LI**nkage of **P**eptides onto **S**caffolds, (*http://www.pepscan.com*), is applicable to peptides in solution as well as on microarrays used for instance for epitope mapping (PEPSCAN method) [26, 27]. Conversion of the peptides is extremely fast (5-10 min) and takes place at room temperature in 100% H_2O at pH 7.8-8.0, or, in case of water-insoluble peptides, in the presence of up to 80% of an organic solvent (ACN, DMF, DMSO). Furthermore, the reactions run smoothly without catalyst and with fully unprotected sidechain functionalities (NH_2, COOH, OH, imidazole, etc.). Occasionally,

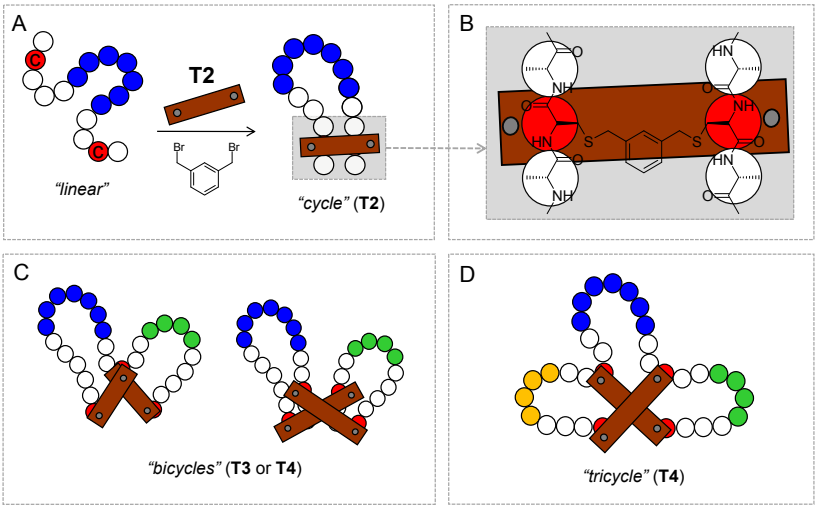

Fig. (3). A) Schematic representation of **CLIPS**-reaction; **B**) molecular structure of **CLIPS**-peptide; **C** and **D**) different **CLIPS**-based topologies (**T3** and **T4**) for mimicry of discontinuous epitopes.

we encounter side reactions at the thioether functionality of methionine, but this is not a general phenomenon and always sequence-dependent.

CLIPS™ technology involves the chemical reaction between peptides containing (homo)cysteine residues and a synthetic scaffold ('**T**' for template) containing a benzyl bromide group ($PhCH_2Br$). Reaction of the **T**-scaffold is entirely selective for the nucleophilic thiol (SH) group of cysteine, and is not observed with amines (NH_2), carboxylic acids (COOH), phenols (PhOH), aliphatic alcohols (RCH_2OH), imidazoles, tryptophans, or thioethers (RCH_2SCH_3). When peptides containing two cysteines are reacted with a scaffold containing two $PhCH_2Br$ groups (*o*-/*m*-/*p*-dibromoxylene, **T2**; 2,6-bis(bromomethyl)pyridine, **P2**), a cyclic product is formed rapidly (Fig. **3AB**). Similarly, reaction of a scaffold containing three (1,3,5-tribromomesitylene, **T3**) or four $PhCH_2Br$ groups (1,2,4,5-tetrabromodurene, **T4**) with peptides containing either three or four cysteines readily produces the corresponding 1:1 products, in which each cysteine has reacted with one of the $PhCH_2Br$ groups, mainly in an intramolecular fashion (Fig. **3CD**). We use **CLIPS™** technology for two main purposes, i.e. *i*) to fix the conformation of linear peptides and so improve antibody binding (mainly **T2**/**P2**), and *ii*) bring together remote parts of discontinuous epitopes in a single, structurally defined entity (mainly **T3**/**T4**). **CLIPS™** technology has found widespread application in 1) epitope mapping studies of therapeutic mAbs [26, 27], 2) eliciting antisera with neutralizing activity for the target protein from which they were derived, and 3) generation and selection of mAbs or scFvs using antibody (hybridoma, phage display library) technologies. Currently, our dataset include more than 50 therapeutically relevant targets, most of which are confidential and proprietary to third parties. Here we present three examples of experimental work that illustrate the kind of results that can be expected when using this technology.

EXAMPLE 1: THE CYS-KNOT PROTEIN FAMILY: FOLLICLE STIMULATING HORMONE (FSH)

Follicle stimulating hormone (FSH) is a hormone that plays a key role in fertility regulation in mammals [28]. Together with luteinizing hormone (LH), thyrotrophin hormone (TSH) and choriogonadotrophin (CG), it constitutes the homologous family of glycoprotein hormones, a subfamily of the cys-knot growth factor superfamily. All four hormones are heterodimers, consisting of a common α-subunit and a unique, hormone-specific β-subunit (Fig. **4A**) [29,30]. *In vivo* neutralization of human-FSH has long been considered a viable option for contraceptive therapy in men [31]. For example, immunization with ovine-FSH has shown to be able to largely impair spermatogenesis and completely inhibit fertility [32]. However, FSH antisera have the potential to crossreact with LH and TSH, which comprise identical α-subunits as FSH. For this reason, peptide vaccines derived from immunization with the FSH-β subunit only have gained increasing interest. Antigenic mapping studies revealed that two of the nine antigenic sites on FSH are located on the β-chain [33]. Moreover, it was shown that residues 31-52 (β2-loop) and 66-85 (β3-loop; Fig. **4B**) harbor epitopes involved in hFSH neutralization. Previous studies in our laboratory showed that sera generated with the tandem β2-loop peptide $(β33\text{-}53)_2$ possessed neutralizing activity. However, similar studies with β3-loop derived peptides were sofar not successful.

Epitope Mapping Studies for Two Neutralizing Anti-FSH mAbs Using CLIPS™ Technology

From a pool of 20 hFSH mAbs, we selected two mAbs (6602 and 5828) with the strongest neutralizing activity against hFSH in a cell-based proliferation assay [34]. Epitope mapping studies using overlapping libraries of 12- to 18-mer **CLIPS** peptides (1-12, 2-13, 3-14, etc.) showed that both mAbs bind to a highly conformational binding site (Fig. **5C**), located mainly at the top of β3-loop (core is R_{62}-L_{73}) [35]. It was found that for 12-mer peptides the binding of **CLIPS** variants was far superior to linear peptides (Fig. **5B**), while for longer peptides (18-mers) the difference in binding levelled off. Apparently, the hydrophobic residues flanking the core region ($_{56}LVY_{58}$ and $_{76}YPV_{78}$) can also serve as a scaffold for loop fixation, e.g. *via* mutual hydrophobic interactions.

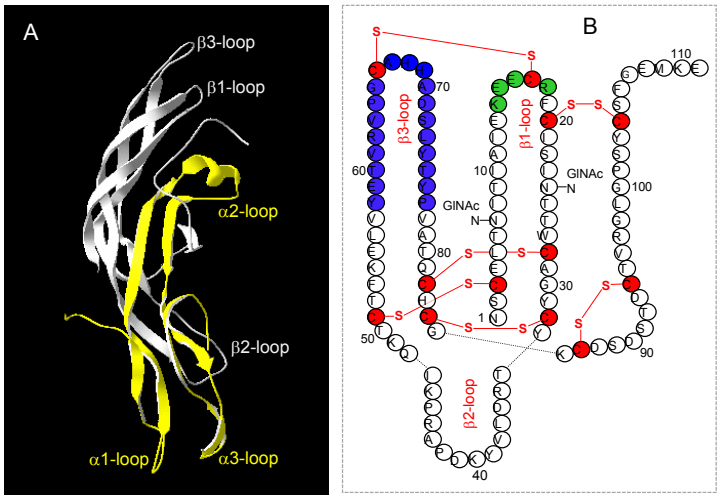

Fig. (4). A) Ribbon structure (1fl7.pdb) of the heterodimeric protein follicle stimulating hormone (FSH), consisting of an α- (in yellow) and β-subunit (in grey); **B**) primary amino acid sequence, loop structures and disulfide topologies in FSH-β.

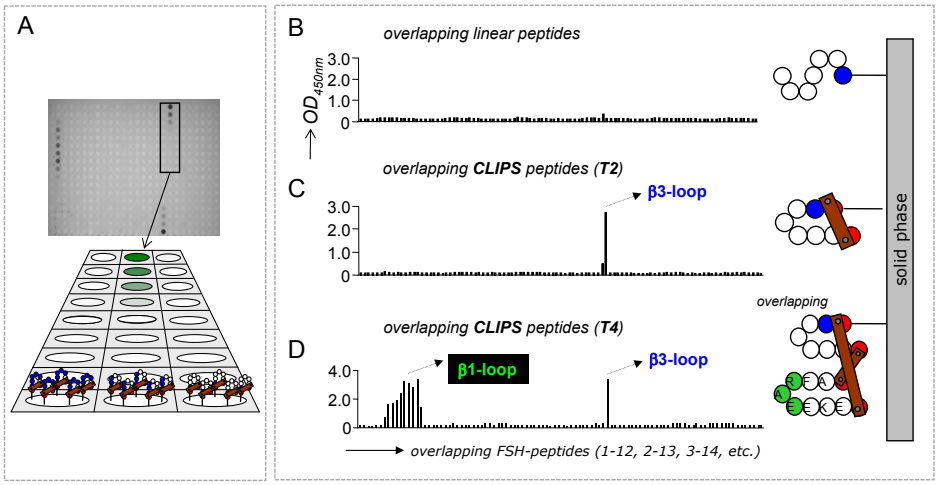

Fig. (5). A) "Real-life" picture and schematic figure of a microarray of overlapping **CLIPS** peptides. **B-D**) Epitope mapping data for anti-FSH mAb in three different formats using **B**) linear peptides, **C**) cyclic **CLIPS** peptides (**T2**), and **D**) bicyclic **CLIPS** peptides (**T4**; formed as mixture of *ortho*-, *meta*-, and *para*-substituted isomers). Optical density data ($OD_{450\ nm}$) relate to an ELISA-type binding assay.

In order to identify additional residues that are part of the binding site for mAb 5828 and 6602, we also screened these mAbs in the so-called "double-loopscan" format with **T4** as a scaffold (Fig. **5D**; unpublished data). Therefore, the **CLIPS**-peptide construct $\mathbf{C}_{\mathbf{T4}}$EKEEARFA$\mathbf{C}_{\mathbf{T4}}$-Br_2, the sequence which was derived from the FSH β1-loop, was chemically linked to a microarray of overlapping FSH-β derived peptides *via* the two reactive CH_2Br groups. In this way the residues E_{16} and R_{18} were identified as part of the discontinuous binding site of mAb 5828 and 6602, since all peptides containing these residues showed clearly improved binding to both mAbs. This showed also that the binding site of both mAbs was both conformational and discontinuous in nature, covering residues on top of both the β3- and β1-loop region.

Immunization Studies with CLIPS Peptides Derived from Human FSH

Subsequently, we studied in detail the possibilities to use **CLIPS** peptides derived from the β3-loop of hFSH for generating antibodies that display *in vitro* hFSH neutralizing activity (Fig. **6**) [35]. Initial experiments with **CLIPS** peptides derived from both FSH and hCG β3-loop were successful in 50% (1 of 2) of the immunized rats, in comparison to 0% (0 of 2) both for the SS-looped and linear variants of these. Based on this finding, we then performed a detailed comparative study with peptides derived from the sequence L_{56}-A_{79} of FSH-β (Fig. **6A**). Unequivocally, these studies revealed the superior ability of the **T2**/SS peptide $\mathbf{C}_{\mathbf{(S-)}}$VYET$\mathbf{C}_{\mathbf{T2}}$RVPGNAHHADSL$\mathbf{C}_{\mathbf{T2}}$TYPV$\mathbf{C}_{\mathbf{(S-)}}$ to raise hFSH-crossreactive antibodies. This peptide comprises both a **T2** module (connecting the two cysteines that replace V_{61} and Y_{74}) and an additional SS bond between the cysteines replacing L_{56} and A_{79}. It raised hFSH-crossreactive antibodies in 100% of the rats (6 of 6), in comparison to 50% (1 of 2) and 0% (0 of 2) for the corresponding **T2** and linear variant. Even though the SS-alone peptides also showed activity in 2 out of 2 animals, the ELISA and neutralization titers were significantly lower in this case. Moreover, we recently observed much larger differences in hFSH crossreactivities between antibodies elicited with **T2**/SS- and SS-peptides when studying longer variants of the FSH β3-loop (unpublished data).

Significant crossreactivity with rFSH (but not with hLH or hCG) was observed for all **CLIPS** antisera (ET_{hFSH}~10xET_{rFSH}). In this respect, the anti-FSH mAb 6602 was superior to any of the **CLIPS** peptide antisera as it did not show any sign of crossreactivity for rFSH (ET<1.0) [35].

There is strong evidence that the activity of the **T2**/SS peptide is a direct result of appropriate fixation of the peptides conformation, as judged from circular dichroism (CD) spectroscopy studies in combination with ELISA-competition studies (Fig. **7**). Despite this marked improvement in mAb-binding of the **T2**/SS peptide compared to linear, it is still orders of magnitude lower than that of intact human FSH. This is likely due to the fact that the β3-loop does not cover the complete epitope of mAb 6602, but only the most important part of it (see also Fig. **5D**).

Systematic variation of the **T2** position in the **T2**/SS peptide (59-76, 60-75, 61-74, 62-73, 63-72) showed that only two (63-72, 61-74) of the five **T2**/SS peptides were able to generate hFSH-crossreactive antibodies in rats (2 of 2; data not shown) [35]. In these cases, both amino acid side chains that were replaced by the **CLIPS** reside in the solvent-shielded hydrophobic core of the protein, while for the remaining three inactive peptides at least one of the two amino acid side chains was located in the solvent-exposed area. Changing the **CLIPS** from m-**T2** to o-**T2**, p-**T2**, to m-**P2** did not have a major impact on antibody generation. Yet, the best results were still obtained with the meta-oriented **T2**-scaffold.

Finally, we observed that immunization with **T2**/SS-peptides for which the configuration of the **CLIPS** cysteines

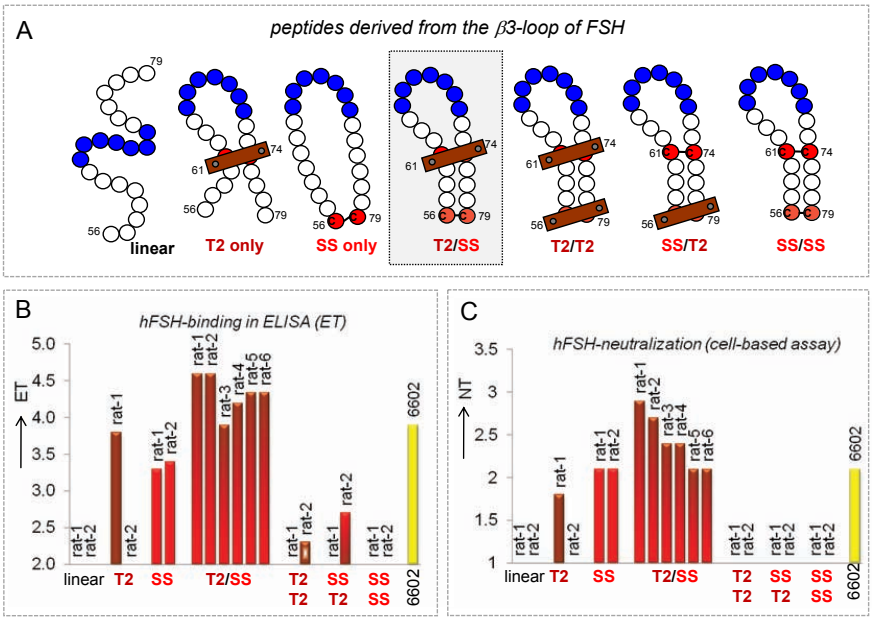

Fig. (6). A) Overview of linear, single- and double-constrained peptides (SS, **T2**, **T2**/SS, SS/SS, etc.) covering the β3-loop sequence L_{56}-A_{79} derived from human FSH-β; **B**) hFSH binding of rat antisera raised with the designated peptides in ELISA (ET = ELISA titer: $-^{10}$log values of serum dilution that gives 4x background OD_{405nm}-level), and **C**) neutralization titer (NT) of rat antisera compared to that of a 10 μg/mL solution of mAb 6602. (NT = $-^{10}$log values of highest serum dilution that shows neutralizing activity; neutralization was measured in Y1 cell-based assay, see [35] for details).

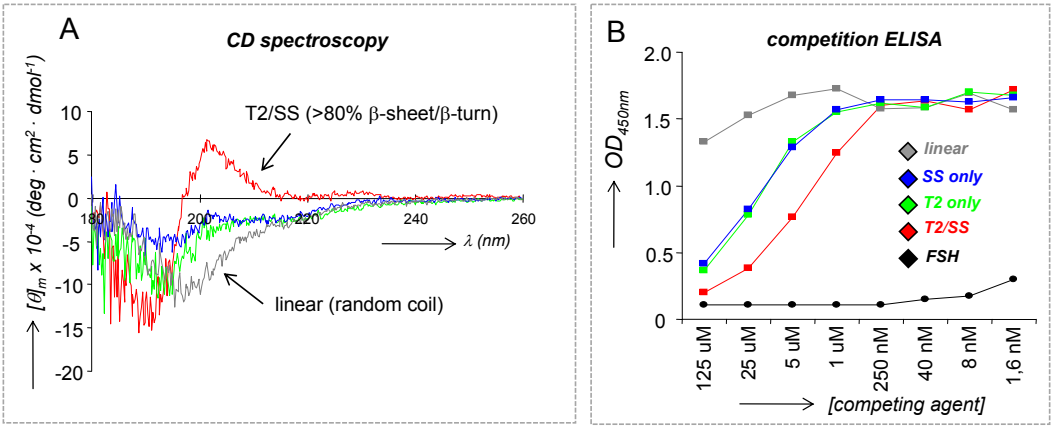

Fig. (7). A) CD spectroscopy measurements of aqueous solutions of linear, SS, **T2** and **T2**/SS peptide derivatives of hFSH β3-loop sequence L_{56}-A_{79}. **B**) Ability of the peptides to inhibit the binding of mAb 5828 to surface-immobilized hFSH. These data provide evidence for the fact that increased structural organization in **T2**/SS is likely to be the reason for improved antigenicity and superior ability to raise hFSH-crossreactive antisera in rats.

was inverted (C_{61}/C_{74}) from L- to D-, either change at a single or both positions, totally prevented the formation of neutralizing antibodies (data not shown) [35]. Crossreactivity with or neutralization of hFSH was no longer observed (ET/NT<1.0) for these antisera. This result is quite interesting in the sense that the **CLIPS** cysteines are not directly involved in antibody binding, but apparently induce a proper orientation of the crucial functionalities (R_{62}, G_{65}, A_{71}, D_{72}, L_{74}). This issue clearly underscores the importance of correct 3-dimensional peptide folding for successful antibody generation and demonstrates that **CLIPS** technology is apparently able to enforce this.

Binding Characteristics of Antisera Elicited with Linear, T2 and T2/SS Peptides

In order to obtain detailed information about the binding mode of the antisera elicited using **CLIPS** peptides, we performed competition experiments with a panel of substitution variants in ELISA [35]. Therefore, we synthesized 28 Ala-replacement (Gly for native Ala) variants of the 32-mer **CLIPS** peptide TFKELVYET**C$_{T2}$**RVPGAAHHADSL**C$_{T2}$** TYPVATQAH (52-83) and investigated the ability of these to effectively block the binding of the various antisera. The competition studies were performed in two different experimental setups, i.e.:

1. using surface-immobilized hFSH (visualizes only "desired" antibodies that crossreact with hFSH).

2. using surface-immobilized **CLIPS** peptide 52-83 (visualizes both "desired" and "undesired" antibodies).

Using these two different formats allowed us to highlight the characteristic differences in binding, i.e. defining the crucial amino acids, between "desired" and "undesired" antibodies.

As a reference, we first studied binding competition for the two neutralizing mAbs (Fig. **8A**). The data showed perfect correlation with replacement studies in peptide microarrays (Fig. **8E**), and identified the amino acids R_{62}, G_{65}, A_{71} (mAb 5828 only), D_{72}, and L_{74} as being crucial for binding. Results obtained with **CLIPS** peptide 52-83 (data not shown) were very similar to the data obtained with surface-immobilized FSH. Only, the observed effects with 52-83 were much less pronounced than with hFSH.

We then studied a selection of peptide antisera, all elicited with β3-loop derived peptides that differ in the extent of structural organization (linear, **T2**, **T2**/SS, Fig. **8B-D**). These data demonstrate how structural organization drastically changes the type of antibodies that is formed. For example, the sera obtained with linear peptides did not show any cross-reactivity with hFSH (Fig. **8B**). Obviously, this is due to the fact that binding occurs mainly at the N- (T_{52}, F_{53}) or C-terminal (Q_{81}, H_{83}) amino acids, which are not solvent-exposed at the hFSH protein surface. With **CLIPS** peptide 52-83 only a small subset of antibodies does crossreact with hFSH (Fig. **8C**, format 1). Interestingly, the crucial amino acids are located mainly in the loop region, with some of these (R_{62}, D_{72}) being identical to those for the neutralizing mAbs. Finally, the antibodies obtained with **CLIPS**/SS peptides show a remarkably close parallel to the neutralizing mAbs 5828 and 6602 with respect to the crucial amino acids. There are some distinct differences (importance of E_{59} and T_{60}), which might be due to steric shielding of these amino acids as a result of glycosylation of FSH. Moreover, there is little to no difference between the data from formats 1 and 2,

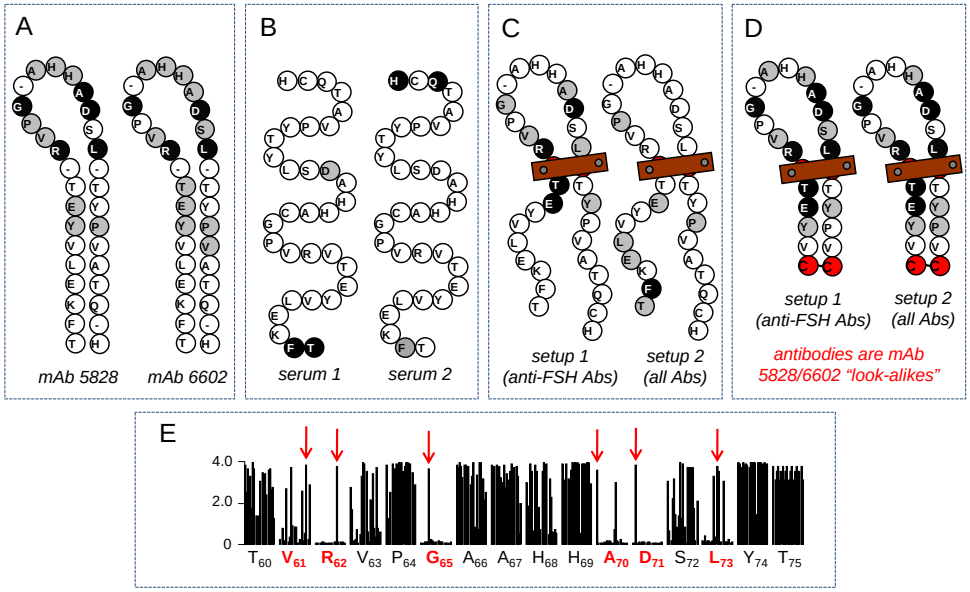

Fig. (8). Overview of the results from ELISA competition experiments with **A**) neutralizing mAbs, **B**) sera elicited with linear peptides (no observed crossreactivity with hFSH), **C**) with **CLIPS** peptides, and **D**) with **CLIPS**/SS peptides. Amino acids in black represent crucial amino acids (>50% inhibition of antibody binding), in grey important (>10% inhibition), and in white not important (<10% inhibition). Ala-replacement variants for cysteines were not included in this study. **E**) Microarray data for binding of mAb 6602 to full replacement analysis of **CLIPS** peptide **C$_{T2}$**TVRVPGAAHHADSLYT**C$_{T2}$**, showing perfect correlation with the data from the ELISA-competition experiments. Black bars are grouped in 16 sets of 19 each. Every bar represents one of 19 substitution variants of all 16 amino acids of **CLIPS** peptide **C$_{T2}$**TVRVPGAAHHADSLYT**C$_{T2}$** that were replaced by all other naturally occurring amino acids (cysteines were not substituted). Red arrows indicate positions of native amino acids.

which proves that the vast majority of generated antibodies is able to bind to hFSH.

EXAMPLE 2: MEMBRANE PROTEINS PART I: THE CD20 ANTIGEN

CD20 is a non-glycosylated 33-37 kD integral plasma membrane protein belonging to the MS4A family. It crosses the plasma membrane four times with both the N- and C-terminus located inside the cell. CD20 is specifically expressed on B cells from pre-B cell until plasmacytoid immunoblast stage (not on lymphoid stem cells and plasma cells) and is found on the surface of >99% of all B-cell lymphomas. Recent evidence confirmed that CD20 plays a role in regulating cell cycling and differentiation as well as being part of a membrane ion-channel [36-38].

Therapeutic successes using monoclonal antibodies (mAbs), either alone or in combination with chemotherapy, continue to raise interest for this relatively new class of drugs. One of the first targets for mAb-therapy was the CD20 antigen, which arguably represents the best validated target for immunotherapy [39]. During the past 10 years, therapeutic mAbs, and in particular the chimeric CD20 antibody rituximab, have changed the treatment paradigm for patients with B-cell neoplasms dramatically [40]. Building on this success, novel CD20 mAbs are being developed which are improved in terms of activity in Fc-dependent effector function and in terms of being fully human [27, 41].

Ofatumumab is a fully human mAb which has demonstrated exceptional activity in preclinical studies [27, 41-43]. It was found to induce stronger complement-dependent cytotoxicity (CDC) than rituximab by promoting more efficient binding of C1q to the surface of CD20-positive cells. Improved activity of this mAb is likely due to the fact that it docks to a different binding site on CD20 and demonstrates a reduced off-rate [39]. Ofatumumab has been shown to have substantial clinical activity as a single agent in the treatment of chronic lymphocytic leukemia and other B cell lymphomas [44-46].

Epitope Mapping Studies for A Series of Mouse and Human CD20 mAbs Using CLIPS™ Technology

In collaboration with GenMab B.V. (Utrecht, The Netherlands) we mapped the binding site of various CD20 mAbs [27]. To this end, we synthesized a set of overlapping **CLIPS** peptides (4-13 amino acids long) covering the extracellular sequences, encompassing amino acid residues 70-84 (small loop) and 140-184 (large loop) of CD20 (Fig. **9A**) and screened these for binding with both human and murine mAbs. Most CD20 mAbs were able to bind well to similar, overlapping, epitopes as measured with both linear and CLIPS peptides. These epitopes encompassed residues A170 and A172, which were previously identified by Polyak and Deans as CD20 mAb epitope by means of mutagenesis studies [47]. However, for ofatumumab, binding was only observed when **CLIPS** peptides were used which, furthermore, revealed completely different binding sites for ofatumumab and the panel of known CD20 mAbs, including rituximab (Fig. **9B**). Most intriguing was the observation that this novel epitope encompassed the small loop (AGIYAPI) of CD20. Based on these data it was concluded that ofatumumab is a unique monoclonal antibody that targets a distinct small loop epitope on the CD20 molecule. It is thought that the close proximity of the epitope to the cell membrane, situates ofatumumab very favorably for inducing complement-dependent cytoxicity. Upon complement activation, short-lived activated complement protein intermediates are generated which can only travel a short distance before they are hydrolyzed. Presumably, the proximal positioning of CD20-ofatumumab-complement protein complexes is then optimal for effective deposition and complement-mediated attack of the tumor cell surface. **CLIPS** mapping of ofatumumab thus identified a novel critical epitope on CD20 and provided important insight into the mechanism of action of this therapeutic antibody.

EXAMPLE 3: MEMBRANE PROTEINS PART II: THE HUMAN CHEMOKINE RECEPTOR CCR5

CC Chemokine receptor 5 (CCR5) is a seven-transmembrane (7TM) chemokine receptor that is part of the

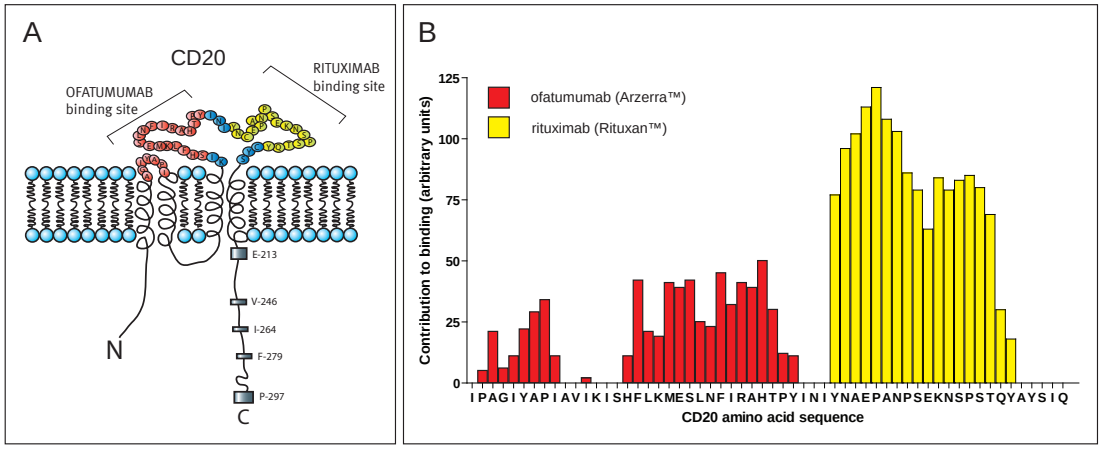

Fig. (9). A) Schematic representation of the two extracellular loops of the membrane-bound CD20 antigen; **B**) Epitope mapping data for ofatumumab (in red) and rituximab (in yellow), showing that both CD20 mAbs bind to a different binding site on CD20. The contribution of CD20 amino acids to binding in B is shown in arbitrary units [27]. It should be noted that the magnitude in AU represents a relative frequency of binding peptides containing the indicated amino acid and not a measure for relative binding strength. The lower bars for ofatumumab thus express a greater selectivity, i.e. it only binds **CLIPS** peptides with proper conformational constraints, whereas rituximab binds a larger proportion of peptides including **CLIPS** as well as linear peptides.

rhodopsin subfamily of G-Protein Coupled Receptors (GPCRs) [48]. It is the major coreceptor for HIV-1 entry [49,50]. CCR5 has been intensely studied since its central role in HIV-1 infection became apparent with the discovery that the absence of CCR5 expression (*via* a homozygous Δ32 deletion) provides resistance to HIV-1 infection [51-53]. CCR5 has been validated as a potential target for prophylaxis against HIV-1 infection and therapy of HIV-1/AIDS [54]. Small-molecule approaches to block the CCR5-HIV interaction have shown promise in clinical trials [55,56], but suffer from the development of resistance [57]. Recent experiments even suggest the future possibility of genetic disruption of CCR5 using zinc-finger nucleases in an attempt to reconstitute immune function in HIV-infected people [58]. Furthermore, anti-CCR5 antibodies are being investigated to block the CCR5-HIV interaction as a potential therapeutic strategy for HIV-1/AIDS [59,60]. A similar approach based on active immunization with GPCR-derived immunogens could have potential as a prophylactic agent for preventing HIV infection [61-63].

Epitope Mapping Studies Using CLIPS™ Technology

In light of this, we tried to reconstruct the binding site of the CCR5-neutralizing mAb 2D7, a CCR5 antibody with strong neutralizing activity [64], by means of **CLIPS** technology. We synthesized overlapping libraries consisting of linear, monocyclic (**T2**) and bicyclic (**T3**) peptides, the sequences of which were all derived from the CCR5-extracellular domain (ECD; Fig. **10A**). In total more than 1500 CLIPS-peptides were screened for binding with 2D7. The results showed that only peptides comprising the ECL2a-derived sequence 170-QKEGLHY-176 displayed affinity for the antibody. Binding was not observed for any of the sequences not incorporating these 7 residues. Moreover, binding of **CLIPS** peptides incorporating 170-QKEGLHY-176 was intense (OD>2; Fig. **10B**) and detectable even at very low antibody concentration (~0.1 μg/mL). In contrast to this, binding of linear peptides was most often not detectable, occasionally only at the highest possible concentration (10 μg/mL).

Detailed mapping studies of the ECL2a-epitope provided valuable information on the mode of antibody binding of mAb 2D7 (Fig. **10C**), nicely complementing the data from Ala-mutation studies with intact CCR5 (Fig. **10D**) [64]. For example, replacement studies on the **CLIPS** peptide 168-$\mathbf{C_{P2}}$RSQKEGLHYT$\mathbf{C_{P2}}$-177 revealed that any replacement of the amino acids K_{171}, E_{172} and G_{173} led to a complete loss of mAb-binding (Fig. **10C**). The amino acid Q_{170} also showed significant decreases in 2D7 binding for most substitutions, albeit with less stringent demands (between 1-2 substitutions tolerated without major loss of binding). Despite this, the peptides with the native amino acids at these positions were still the strongest binders of all. Moreover, **CLIPS** peptide 170-$\mathbf{C_{P2}}$QKEGLHY$\mathbf{C_{P2}}$-176 was found to be the shortest possible sequence showing binding to 2D7 (data not shown), which is indicative for the importance of both Q_{170} and Y_{176} for binding. The relatively low sensitivity to substitution of Y_{176} can be best explained by assuming a conformational role for this amino acid, which somehow may interact with one of the crucial amino acids by positioning the side chains of these in the correct orientation for binding. This seems fully in accordance with the fact that Y_{176} was not identified as a crucial amino acid in Ala-mutation studies on intact CCR5 (Fig. **10C**) [64].

All other amino acids (T_{167}, R_{168}, L_{174}, H_{175}, T_{177}) showed a very low level of resistance to substitution (>10 substitutions tolerated), most likely indicating that they do not specifically interact with the antibody. For some of these, significant binding improvements were observed upon substitution with others (L_{174}/Q, H_{175}/N, T_{176}/FIKL), which might be due to the fact that the native amino acids stabilize conformations of the peptides that are suboptimal for 2D7 binding.

Competition ELISA Studies with CLIPS Peptides Derived from ECL2a

In order to confirm the mapping data we performed a series of ELISA competition experiments. Moreover, we wanted to address in more detail the effect of conformational

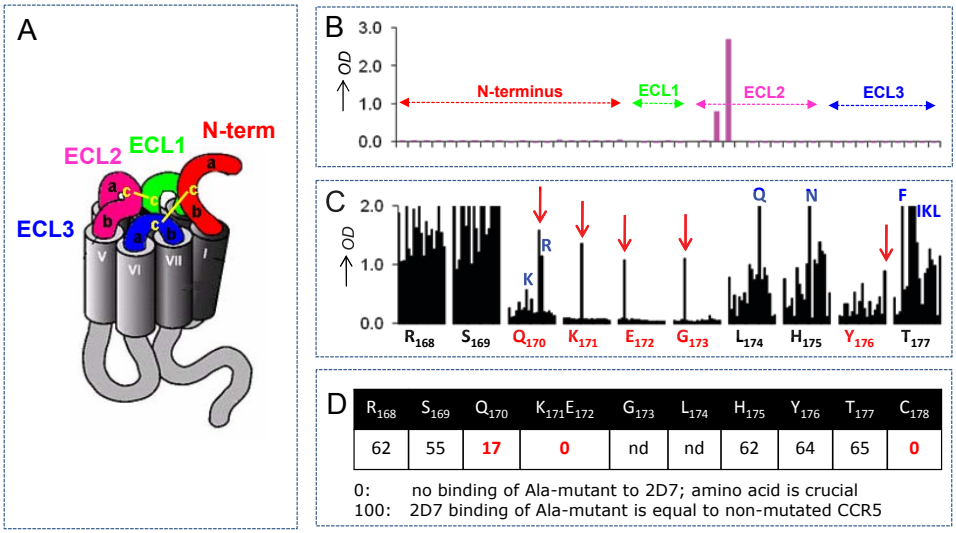

Fig. (10). **A**) Schematic illustration of a GPCR, **B**) Epitope mapping data for mAb 2D7 using overlapping libraries of CLIPS peptides derived from the ECL domain of CCR5, **C**) binding data for mAb 2D7 to a full replacement analysis of **CLIPS** peptide *$\mathbf{C_{P2}}$RSQKEGLHYT$\mathbf{C_{P2}}$ (red arrows indicate native amino acids), and **D**) data from Ala-mutation studies on intact CCR5 [64].

fixation of the peptides on mAb 2D7 binding. Therefore, we studied the ability of various ECL2a-derived peptides to inhibit the binding of mAb 2D7 to a surface-immobilized CCR5 antigen. We used the **CLIPS** peptide $\mathbf{C}_{(S-)}$FTR$\mathbf{C}_{T2}$QKEGLHYT$\mathbf{C}_{T2}$SSH$\mathbf{C}_{(S-)}$ (purified by HPLC) for surface-immobilization as a valuable substitute for CCR5, since purified CCR5 is not available as it is an integral membrane protein. We compared two sets of peptides. In the first set, we studied the effect of conformational fixation (linear, **T2** and **T2**/SS) on binding (Fig. **11A** and **B**). Secondly, we compared the effect of substituting one (mimic-1) or several (mimics 2-3) of the (non-essential) native amino acids on 2D7 binding (Fig. **11C** and **D**).

The competition data confirm the results from the epitope mapping and replacement analysis studies. The linear peptide TRSQKEGLHYTSGSC did not show any competition at all, not even at the highest concentration used (500 μM; Fig. **11B**). In contrast to this, the **T2**-constrained peptide TR$\mathbf{C}_{T2}$QKEGLHYT$\mathbf{C}_{T2}$GSC clearly showed activity (>50% competition) at 500 μM. Finally, the **T2**/SS $\mathbf{C}_{(S-)}$R$\mathbf{C}_{T2}$QKEGLHYT$\mathbf{C}_{T2}$SC$_{(S-)}$ proved most active of all three, showing an ~80% decrease in binding of 2D7 at 165 μM. Replacement of some of the amino acids in **T2**-peptide TR$\mathbf{C}_{T2}$QKEGLHYT$\mathbf{C}_{T2}$GSC, previously identified as non-essential, also improved the ability to reduce 2D7 binding (Fig. **11C** and **D**). Mimic-1 (Q_{170}/R only) and -2 (4 replacements: Q_{170}/R, L_{174}/Q, H_{175}/N, and T_{177}/I) showed improved activity compared to native **T2**-peptide, in particular at the two highest concentrations (500 and 160 μM). For mimic-3 (only 3 replacements: L_{174}/Q, H_{175}/N, and T_{177}/I) the improved activity in competition was still visible at 18 μM, which confirmed our earlier finding that Q_{170} is important for 2D7 binding. The improved activity is likely due to replacement of either L_{174}, H_{175}, or T_{177}, or a combination of these.

Antibody Generation Using CLIPS™ Technology

In a pilot study, we investigated the potential of the strongest binding ECL2a-derived **CLIPS** peptides to generate antibodies capable of neutralizing the bioactivity of CCR5. We included 2 different ECL2a-mimics (1/2) in two different formats (1/2 or 1*/2*) and two mimics derived from the N-terminus (mimic 4: MDYQVSSPIY-DINYYTSEP$\mathbf{C}_{T2}$QKINVK$\mathbf{C}_{T2}$) and the N-terminus + ECL1 (mimic 5: MDYQVSSPIYDINYYTSEP$\mathbf{C}_{T3}$QKINVK$\mathbf{C}_{T3}$ AAQWDFGNTM$\mathbf{C}_{T3}$). ECL2a-mimics 1-2 all have incorporated 1 (mimic 1: TR$\mathbf{C}_{T2}$**R**KEGLHYT$\mathbf{C}_{T2}$) or 4 (mimic 2: TR$\mathbf{C}_{T2}$**R**KEG**QN**Y**I**C$_{T2}$) amino acid replacements in comparison to the native ECL2a-sequence (167-TRSQKEGLH-YTC-178). Mimics 1/2 and 1*/2* differ only in the mode of conjugation to the carrier protein (KLH), i.e. either *via* a C-terminal extension (GSC-sequence; mimics 1/2) or *via* the use of an SH-functionalized **T2** scaffold (mimics 1*/2*). BALB/c mice were immunized (4 mice per mimic) and the sera were tested for CCR5-positive staining in flow cytometry (Fig. **12A**).

The sera from ECL2a mimic-2 gave by far the best results (3 of 4 sera CCR5-positive). Splenocytes were isolated from all four CCR5-positive mice and used to generate hybridomas. 180 viable mAbs were selected, from which 32 produced antibodies that showed positive staining for CCR5 in flow cytometric analysis (Multispan, Hayward, CA, USA; Fig. **12B**). The charts for mAb 2D7 and mAb 9 at two different concentrations (~1 and 0.1 ug/mL) are shown (Fig. **12C** and **D**).

In summary, these data show the potential of **CLIPS** peptide mimics to generate mAbs for GPCRs, in particular for CCR5. Even though the data were not optimized for the application, this example provides a good perspective of what might be achievable for related GPCRs or even for

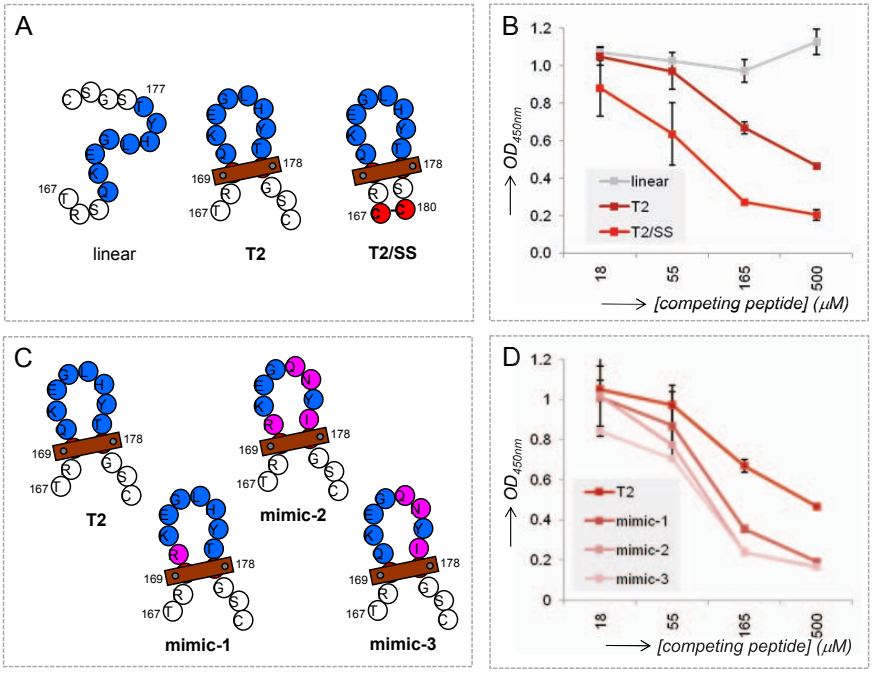

Fig. (11). Competition studies in ELISA with two different sets of peptides derived from the ECL2a sequence 167-TRSQKEGLHYTC-178; **A-B**) results for linear, **T2** and **T2**/SS constrained peptides; **C-D**) results for **T2** peptide TR$\mathbf{C}_{T2}$QKEGLHYT$\mathbf{C}_{T2}$GSC and corresponding mimics 1 (Q_{170}/R), 2 (Q_{170}/R; L_{174}/Q; H_{175}/N; T_{177}/I) and 3 (L_{174}/Q; H_{175}/N; T_{177}/I). ELISA-measurements were performed in duplicate.

A

Nr.	CCR5 domain	GPCR positive in FACS*	fusion
1	ECL2a	1 of 4	-
2	ECL2a	3 of 4	mice 1-3
1*	ECL2a	1 of 4	-
2*	ECL2a	1 of 4	-
4	Nterm	1 of 4	mouse 4
5	Nterm + ECL1	0 of 4	-

B

Mouse	viable mAbs	GPCR positive in FACS*
1	37	7
2	14	1
3	120	23
4	9	1 (mAb 9)

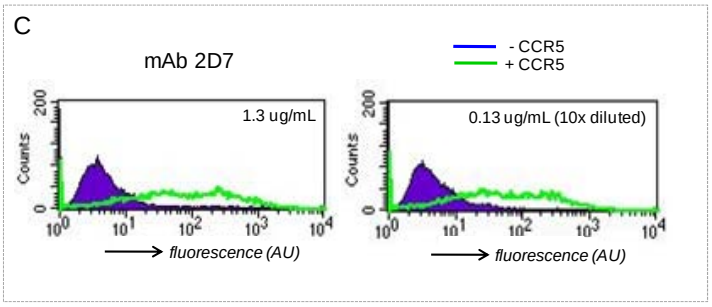

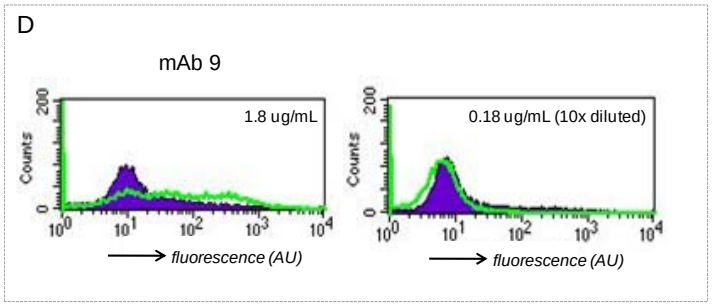

Fig. (12). Overview of results from flow cytrometric analysis on CCR5-expressing cells for **A**) antisera elicited with six different CCR5-mimics, **B**) 180 viable hybridoma clones generated with splenocytes from mice with CCR5-positive antisera. Flow cytometry data for **C**) mAb 2D7 (positive control) and **D**) mAb 9. Binding of mAb 2D7 and mAb 9 to CCR5-expression cells (+ CCR5) was detected by an anti-mouse IgG1-FITC conjugate. As a control, background binding was assessed on CCR5 negative non-transfected cells (- CCR5).

structurally more complicated membrane-bound proteins (e.g. ion-channels).

CONCLUSIONS AND FUTURE PERSPECTIVES

In conclusion, **CLIPS™** technology proves to be useful in protein binding site reconstruction, not only for epitope mapping purposes, but more importantly also to raise neutralizing antibodies. The technology is particularly attractive for its ease of application, the extremely fast and clean conversions of the peptides involved, and the mild reaction conditions combined with the chemical robustness of the cyclised peptides. Application of this technology to map mAbs against therapeutically relevant targets (hFSH, hCG, CD20, and CCR5) illustrates clearly how the technology can be used to define binding sites at the single amino acid level. The work presented holds great promise for application to other protein targets, in particular those with considerable structural complexity (ion-channels, viruses).

ACKNOWLEDGEMENTS

We thank Dr. Stephen Carlisle from Unipath Limited (UK) for providing the anti-FSH mAbs 5828 and 6602.

REFERENCES

[1] Fairlie, D.P.; West, M.L.; Wong, A.K. Towards protein surface mimetics. *Curr. Med. Chem.*, **1998**, *5*(1), 29-62.

[2] Waldmann, T.A. Immunotherapy: past, present and future. *Nat. Med.*, **2003**, *9*(3), 269-277.

[3] Adams, G.P.; Weiner, L.M. Monoclonal antibody therapy of cancer. *Nat. Biotechnol.*, **2005**, *23*(9), 1147-1157.

[4] Bittle, J.L.; Houghton, R.A.; Alexander, H.; Shinnick, T.M.; Sutcliffe, J.G.; Lerner, R.A.; Rowlands, D.J.; Brown, F. Protection against foot-and-mouth disease by immunization with a chemically synthesized peptide predicted from the viral nucleotide sequence. *Nature*, **1982**, *298*(5869), 30-33.

[5] DiMarchi, R.; Brooke, G.; Gale, C.; Cracknell, V.; Doel, T.; Mowat, N. Protection of cattle against foot-and-mouth disease by a synthetic peptide. *Science*, **1986**, *232*(4750), 639-641.

[6] Langeveld, J.P.M.; Casal, J.I.; Osterhaus, A.D.; Cortés, E.; de Swart, R.; Vela, C.; Dalsgaard, K.; Puijk, W.C.; Schaaper, W.M.M.; Meloen, R.H. First peptide vaccine providing protection against viral-infection in the target animal - studies of canine parvovirus in dogs. *J. Virol.*, **1994**, *68*(7), 4506-4513.

[7] Langeveld, J.P.M.; Casal, J.I.; Cortés, E.; van de Wetering, G.; Boshuizen, R.S.; Schaaper, W.M.M.; Dalsgaard, K.; Meloen, R.H. Effective induction of neutralizing antibodies with the amino-terminus of VP2 of canine parvovirus as a synthetic peptide. *Vaccine*, **1994**, *12*(15), 1473-1480.

[8] Talwar, G.P. Vaccines for control of fertility and hormone-dependent cancers. *Immunol. Cell Biol.*, **1997**, *75*(2), 184-189.

[9] Naz, R.K.; Gupta, S.K.; Gupta, J.C.; Vyas, H.K.; Talwar, G.P. Recent advances in contraceptive vaccine development: a mini-review. *Hum. Reprod.*, **2005**, *20*(12), 3271-3283.

[10] Moulton, H.M.; Yoshihara, P.H.; Mason, D.H.; Iversen, P.L.; Triozzi, P.L. Active specific immunotherapy with a beta-human chorionic gonadotropin peptide vaccine in patients with metastatic colorectal cancer: Antibody response is associated with improved survival. *Clin. Cancer Res.*, **2002**, *8*(7), 2044-2051.

[11] Iversen, P.L.; Mourich, D.V.; Moulton, H.M. Monoclonal antibodies to two epitopes of beta-human chorionic gonadotropin for the treatment of cancer. *Curr. Opin. Mol. Ther.*, **2003**, *5*(2), 156-160.

[12] Mutter, M.; Dumy, P.; Garrouste, P.; Lehmann, C.; Mathieu, M.; Peggion, C.; Peluso, S.; Razaname, A.; Tuchscherer, G. Template assembled synthetic proteins (TASP) as functional mimetics of proteins. *Angew. Chem. Int. Ed. Eng.*, **1996**, *35*(13/14), 1482-1485.

[13] Kuwabara, I.; Maruyama, H.; Kamisue, S.; Shima, M.; Yoshioka, A.; Maruyama, I.N. Mapping of the minimal domain encoding a conformational epitope by λ phage surface display: factor VIII inhibitor antibodies from haemophilia A patients. *J. Immunol. Methods*, **1999**, *224*(1/2), 89-99.

[14] Cui, X.; Nagesha, H.S.; Holmes, I.H. Mapping of conformational epitopes on capsid protein VP2 of infectious bursal disease virus by fd-tet phage display. *J. Virol. Methods*, **2003**, *114*(1), 109-112.

[15] Mutter, M.; Vuilleumier, S. A chemical approach to protein design – template-assembled synthetic proteins (TASP). *Angew. Chem. Int. Ed. Engl.*, **1989**, *28*(5), 535-554.

[16] Blackwell, H.E.; Grubbs, R.H. Highly efficient synthesis of covalently cross-linked peptide helices by ring-closing metathesis. *Angew. Chem. Int. Ed. Engl.*, **1998**, *37*(23), 3281-3284.

[17] Karle, I.L. Aspects of peptide folding and aggregation. *Acc. Chem. Res.*, **1999**, *32*(8), 693-701.

[18] Orner, B.P.; Salvatella, X.; Sánchez Quesada, J.; de Mendoza, J.; Giralt, E.; Hamilton, A.D. De novo protein surface design: Use of cation-π interactions to enhance binding between an α-helical peptide and a cationic molecule in 50% aqueous solution. *Angew. Chem. Int. Ed. Engl.*, **2002**, *41*(1), 117-119.

[19] Walensky, L.D.; Kung, A.L.; Escher, I.; Malia T.J.; Barbuto, S.; Wright, R.D.; Wagner G.; Verdine, G.L.; Korsmeyer S.J. Activation of apoptosis *in vivo* by a hydrocarbon-stapled BH3 helix. *Science*, **2004**, *305*(5689), 1466-1470.

[20] Nowick, J.S. Chemical models of protein β-sheets. *Acc. Chem. Res.*, **1999**, *32*(4), 287-296.

[21] Burgess, K. Solid-phase syntheses of β-turn analogues to mimic or disrupt protein-protein interactions. *Acc. Chem. Res.*, **2001**, *34*(10), 826-835.

[22] Cochran, A.G.; Skelton, N.J.; Starovasnik, M.A. Tryptophan zippers: stable, monomeric beta-hairpins. *Proc. Natl. Acad. Sci. USA*, **2001**, *98*(10), 5578-5583.

[23] Löwik, D.; Linhardt, J.G.; Adams, P.J.; van Hest, J.C.M. Non-covalent stabilization of a beta-hairpin peptide into liposomes. *Org. Biomol. Chem.*, **2003**, *1*(11), 1827-1829.

[24] Reichwein, J.F.; Wels, B.; Kruijtzer, J.A.W.; Versluis, C.; Liskamp, R.M.J. Rolling loop scan: An approach featuring ring-closing metathesis for generating libraries of peptides with molecular shapes mimicking bioactive conformations or local folding of peptides and proteins. *Angew. Chem. Int. Ed. Engl.*, **1999**, *38*(24), 3684-3687.

[25] Angell, Y.L.; Burgess, K. Peptidomimetics *via* copper-catalyzed azide-alkyne cycloadditions. *Chem. Soc. Rev.*, **2007**, *36*(10), 1674-1689.

[26] Timmerman, P.; Beld, J.; Puijk, W.C.; Meloen, R.H. Rapid and quantitative cyclization of multiple peptide loops onto synthetic scaffolds for structural mimicry of protein surfaces. *Chembiochem*, **2005**, *6*(5), 821-824.

[27] Teeling, J.L.; Mackus, W.J.M.; Wiegman, L.J.J.M.; van den Brakel, J.H.N.; Beers, S.A.; French, R.R.; van Meerten, T.; Ebeling, S.; Vink, T.; Slootstra, J.W.; Parren, P.W.H.I.; Glennie, M.J.; van de Winkel, J.G.J. The biological activity of human CD20 monoclonal antibodies is linked to unique epitopes on CD20. *J. Immunol.*, **2006**, *177*(1), 362-371.

[28] Pierce, J.G.; Parsons, T.F. Glycoprotein hormones: structure and function. *Annu. Rev. Biochem.*, **1981**, *50*, 465-495.

[29] Fox, K.M.; Dias, J.A.; van Roey, P. Three-dimensional structure of human follicle-stimulating hormone. *Mol. Endocrinol.*, **2001**, *15*(3), 378-389.

[30] Fan, Q.R.; Hendrickson, W.A. Structure of human follicle-stimulating hormone in complex with its receptor. *Nature*, **2005**, *433*(7023), 269-277.

[31] Moudgal, N.R.; Jeyakumar, M.; Krishnamurthy, H.N.; Sridhar, S.; Krishnamurthy, H.; Martin, F. Development of male contraceptive vaccine - a perspective. *Hum. Reprod. Update*, **1997**, *3*(4), 335-346.

[32] Moudgal, N.R.; Ravindranath, N.; Murthy, G.S.; Dighe, R.R.; Aravindan, G.R.; Martin, F. Long term contraceptive efficacy of vaccine of ovine follicle-stimulating hormone in male bonnet monkeys (*macaca radiata*). *J. Reprod. Fertil.*, **1992**, *96*(1), 91-102.

[33] Berger, P.; Panmoung, W.; Khaschabi, D.; Mayregger, B.; Wick, G. Antigenic features of human follicle-stimulating hormone delineated by monoclonal antibodies and construction of an immunoradiomometric assay. *Endocrinol.*, **1988**, *123*(5), 2351-2359.

[34] Timmerman, P.; van Dijk, E.; Puijk, W.; Schaaper, W.; Slootstra, J.; Carlisle, S.J.; Coley, J.; Eida, S.; Gani, M.; Hunt, T.; Perry, P.; Piron, G.; Meloen, R.H. Mapping of a discontinuous and highly conformational binding site on follicle stimulating hormone subunit-β (FSH-β) using domain scan and matrix scan technology. *Mol. Divers.*, **2004**, *8*(2), 61-77.

[35] Timmerman, P.; Puijk, W.C.; Meloen, R.H. Functional reconstruction and synthetic mimicry of a conformational epitope using CLIPS™ technology. *J. Mol. Recognit.*, **2007**, *20*(5), 283-299.

[36] Tedder, T.F.; Engel, P. CD20: a regulator of cell-cycle progression of B lymphocytes. *Immunol. Today*, **1994**, *15*(9), 450-454.

[37] Polyak, M.J.; Li, H.; Shariat, N.; Deans, J.P. CD20 homo-oligomers physically associate with the B cell antigen receptor; dissociation upon receptor engagement and recruitment of phosphoproteins and calmodulin binding proteins. *J. Biol. Chem.*, **2008**, *283*(27), 18545-18552.

[38] Walshe, C.A.; Beers, S.A.; French, R.R.; Chan, C.H.T.; Johnson, P.W.; Packham, G.K.; Glennie, M.J.; Cragg, M.S. Induction of cytosolic calcium flux by CD20 is dependent upon B cell antigen receptor signaling. *J. Biol. Chem.*, **2008**, *283*(25), 16971-16984.

[39] Castillo, J.; Winer, E.; Quesenberry, P. Newer monoclonal antibodies for hematological malignancies. *Exp. Hematol.*, **2008**, *36*(7), 755-768.

[40] Coiffier, B. Rituximab therapy in malignant lymphoma. *Oncogene*, **2007**, *26*(25), 3603-3613.

[41] Teeling, J.L.; French, R.R.; Cragg, M.S.; van den Brakel, J.; Pluyter, M.; Huang, H.; Chan, C.; Parren, P.W.H.I.; Hack, C.E.; Dechant, M.; Valerius, T.; van de Winkel, J.G.J.; Glennie, M.J. Characterization of new human CD20 monoclonal antibodies with potent cytolytic activity against non-Hodgkin lymphomas. *Blood*, **2004**, *104*(6), 1793-1800.

[42] Bleeker, W.K.; Munk, M.E.; Mackus, W.J.M.; van den Brakel, J.H.N.; Pluyter, M.; Glennie, M.J.; van de Winkel, J.G.J.; Parren, P.W.H.I. Estimation of dose requirements for sustained *in vivo* activity of a therapeutic human anti-CD20 antibody. *Br. J. Haematol.*, **2008**, *140*(3), 303-312.

[43] Beum, P.V.; Lindorfer, M.A.; Beurskens, F.; Stukenberg, P.T.; Lokhorst, H.M.; Pawluczkowycz, A.W.; Parren, P.W.H.I.; van de Winkel, J.G.J.; Taylor, R.P. Complement activation on B lymphocytes opsonized with rituximab or ofatumumab produces substantial changes in membrane structure preceding cell lysis. *J. Immunol.*, **2008**, *181*(1), 822-832.

[44] Hagenbeek, A.; Gadeberg, O.; Johnson, P.; Pedersen, L.M.; Walewski, J.; Hellmann, A.; Link, B.K.; Robak, T.; Wojtukiewicz, M.; Pfreundschuh, M.; Kneba, M.; Engert, A.; Sonneveld, P.; Flensburg, M.; Petersen, J.; Losic, N.; Radford, J. First clinical use of ofatumumab, a novel fully human anti-CD20 monoclonal antibody in relapsed or refractory follicular lymphoma: results of a phase 1/2 trial. *Blood*, **2008**, *111*(12), 5486-5495.

[45] Coiffier, B.; Lepretre, S.; Pedersen, L.M.; Gadeberg, O.; Fredriksen, H.; van Oers, M.H.J.; Wooldridge, J.; Kloczko, J.; Holowiecki, J.; Hellmann, A.; Walewski, J.; Flensburg, M.; Petersen, J.; Robak, T. Safety and efficacy of ofatumumab, a fully human monclonal anti-CD20 antibody, in patients with relapsed or refractory B-cell chronic lymphocytic leukemia: a phase 1-2 study. *Blood*, **2008**, *111*(3), 1094-1100.

[46] Osterborg, A.; Kipps, T.J.; Mayer, J.; Stilgenbauer, S.; Williams, C.D.; Hellmen, A.; Robak, T.; Furman, R.R; Hillmen, P.; Trneny, M.; Dyer, M.J.S.; Padmanabhan, S.; Kozak, T.; Chan, G.; Davis, R.L.; Losic, N.; Russell, C.A.; Piotrowska, M.; Wilms, J.; Wierda, W.G. Ofatumumab (HuMax-CD20), a novel monoclonal antibody, is an active treatment for patients with CLL refractory to both fludarabine and alemtuzumab or bulky fludarabine-refractory disease: results from the planned interim analysis of an international pivotal trial. *Blood*, **2008**, *112*(126), 328-328.

[47] Polyak, M.J.; Deans, J.P. Alanine-170 and proline-172 are critical determinants for extracellular CD20 epitopes; heterogeneity in the fine specificity of CD20 monoclonal antibodies is defined by additional requirements imposed by both amino acid sequence and quaternary structure. *Blood*, **2002**, *99*(9), 3256-3262.

[48] Bockaert, J.; Claeysen, S.; Bécamel, C.; Pinloche, S.; Dumuis, A. G protein-coupled receptors: dominant players in cell-cell communication. *Int. Rev. Cytol.*, **2002**, *212*, 63-132.

[49] Deng, H.K.; Liu, R.; Ellmeier, W.; Choe, S.; Unutmaz, D.; Burkhart, M.; DiMarzio, P.; Marmon, S.; Sutton, R.E.; Hill, C.M.; Davis, C.B.; Peiper, S.C.; Schall, T.J.; Littman, D.R.; Landau, N.R. Identification of a major co-receptor for primary isolates of HIV-1. *Nature*, **1996**, *381*(6584), 661-666.

[50] Atchison, R.E.; Gosling, J.; Monteclaro, F.S.; Franci, C.; Digilio, L.; Charo, I.F.; Goldsmith, M.A. Multiple extracellular elements of CCR5 and HIV-1 entry: dissociation from response to chemokines. *Science*, **1996**, *274*(5294), 1924-1926.

[51] Liu, R.; Paxton, W.A.; Choe, S.; Cerandini, D.; Martin, S.R.; Horuk, R.; MacDonald, M.E.; Stuhlmann, H.; Koup, R.A.; Landau, N.R. Homozygous defect in HIV-1 coreceptor accounts for resistance of some multiply-exposed individuals to HIV-1 infection. *Cell*, **1996**, *86*(3), 367-377.

[52] Samson, M.; Libert, F.; Doranz, B.J.; Rucker, J.; Liesnard, C.; Farber, C.M.; Saragosti, S.; Lapoumeroulie, C.; Cognaux, J.; Forceille, C.; Muyldermans, G.; Verhofstede, C.; Burtonboy, G.; Georges, M.; Imai, T.; Rana, S.; Yi, Y.; Smyth, R.J.; Collman, R.G.; Doms, R.W.; Vassart, G.; Parmentier, M. Resistance to HIV-1 infection in caucasian individuals bearing mutant alleles of the CCR-5 chemokine receptor gene. *Nature*, **1996**, *382*(6593), 722-725.

[53] Huang, Y.; Paxton, W.A.; Wolinsky, S.M.; Neumann, A.U.; Zhang, L.; He, T.; Kang, S.; Ceradini, D.; Jin, Z.; Yazdanbakhsh, K.; Kunstman, K.; Erickson, D.; Dragon, E.; Landau, N.R.; Phair, J.; Ho, D.D.; Koup, R.A. The role of a mutant CCR5 allele in HIV-1 transmission and disease progression. *Nat. Med.*, **1996**, *2*(11), 1240-1243.

[54] Lederman, M.M.; Veazey, R.S.; Offord, R.; Mosier, D.E.; Dufour, J.; Mefford, M.; Piatak, M.; Lifson, J.D.; Salkowitz, J.R.; Rodriguez, B.; Blauvelt, A.; Hartley, O. Prevention of vaginal SHIV transmission in rhesus macaques through inhibition of CCR5. *Science*, **2004**, *306*(5695), 485-487.

[55] Fätkenheuer, G.; Pozniak, A.L.; Johnson, M.A.; Plettenberg, A.; Staszewski, S.; Hoepelman, A.I.; Saag, M.S.; Goebel, F.D.; Rockstroh, J.K.; Dezube, B.J.; Jenkins, T.M.; Medhurst, C.; Sullivan, J.F.; Ridgway, C.; Abel, S.; James, I.T.; Youle, M.; Van der Ryst, E. Efficacy of short-term monotherapy with maraviroc, a new CCR5 antagonist, in patients infected with HIV-1. *Nat. Med*., **2005**, *11*(11), 1170-1172.

[56] Abad, J.L.; Gonzalez, M.A.; Del Real, G.; Mira, E.; Manes, S.; Serrano, F. Bernad, A. Novel interfering bifunctional molecules against the CCR5 coreceptor are efficient inhibitors of HIV-1 infection. *Mol. Ther.*, **2003**, *8*(3), 475-484.

[57] Kuhmann, S.E.; Pugach, P.; Kunstman, K.J.; Taylor, J.; Stanfield, R.L.; Snyder, A.; Strizki, J.M.; Riley, J.; Baroudy, B.M.; Wilson, I.A.; Korber, B.T.; Wolinsky, S.M.; Moore, J.P. Genetic and phenotypic analyses of human immunodeficiency virus type 1 escape from a small-molecule CCR5 inhibitor. *J. Virol.*, **2004**, *78*(6), 2790-2807.

[58] Perez, E.E.; Wang, J.; Miller, J.C.; Jouvenot, Y.; Kim, K.A.; Liu, O.; Wang, N.; Lee, G.; Bartsevich, V.V.; Lee, Y.L.; Guschin, D.Y.; Rupniewski, I.; Waite, A.J.; Carpenito, C.; Carroll, R.G.; Orange, J.S.; Urnov, F.D.; Rebar, E.J.; Ando, D.; Gregory, P.D.; Riley, J.L.; Holmes, M.C.; June, C.H. Establishment of HIV-1 resistance in CD4(+) T cells by genome editing using zinc-finger nucleases. *Nat. Biotechnol.*, **2008**, *26*(7), 808-816.

[59] Trkola, A.; Ketas, T.J.; Nagashima, K.A.; Zhao, L.; Cilliers, T.; Morris, L.; Moore, J.P.; Maddon, P.J.; Olson, W.C. Potent, broad-spectrum inhibition of human immunodeficiency virus type 1 by the CCR5 monoclonal antibody PRO 140. *J. Virol.*, **2001**, *75*(2), 579-588.

[60] Jacobsen, J.M.; Saag, M.S.; Thompson, M.A.; Fischl, M.A.; Liporace, R.; Reichmann, R.C.; Redfield, R.R.; Fichtenbaum, C.J.; Zingman, B.S.; Patel, M.C.; Murga, J.D.; Pemrick, S.M.; D'Ambrosio, P.; Michael, M.; Kroger, H.; Ly, H.; Rotshteyn, Y.; Buice, R.; Morris, S.A.; Stavola, J.J.; Maddon, P.J.; Kremer, A.B.; Olson, W.C. Antiviral activity of single-dose PRO140, a CCR5 monoclonal antibody, in HIV-infected adults. *J. Infect. Dis.*, **2008**, *198*(9), 1345-1352.

[61] Chackerian, B.; Lowy, D.R.; Schiller, J.T. Induction of autoantibodies to mouse CCR5 with recombinant papillomavirus particles. *Proc. Natl. Acad. Sci. USA*, **1999**, *96*(5), 2373-2378.

[62] Lehner, T.; Doyle, C.; Wang, Y.; Babaahmady, K.; Whittall, T.; Tao, L.; Bergmeier, L.; Kelly, C. Immunogenicity of the extracellular domains of C-C chemokine receptor 5 and the *in vitro* effects on simian immunodeficiency virus or HIV infectivity. *J. Immunol.*, **2001**, *166*(12), 7446-7455.

[63] Misumi, S.; Nakajima, R.; Takamune, N.; Shoji, S. A cyclic dodecapeptide-multiple-antigen peptide conjugate from the undecapeptidyl arch (from Arg_{168} to Cys_{178}) of extracellular loop 2 in CCR5 as a novel human immunodeficiency virus type 1 vaccine. *J. Virol.*, **2001**, *75*(23), 11614-11620.

[64] Olson, W.C.; Rabut, G.E.E.; Nagashima, K.A.; Tran, D.N.H.; Anselma, D.J.; Monard, S.P.; Segal, J.P.; Thompson, D.A.D.; Kajumo, F.; Guo, Y.; Moore, J.P.; Maddon, P.J.; Dragic, T. Differential inhibition of human immunodeficiency virus type 1 fusion, gp120 binding, and CC-chemokine activity by monoclonal antibodies to CCR5. *J. Virol.*, **1999**, *73*(5), 4145-4155.

Received: December 12, 2008 Revised: April 24, 2009 Accepted: April 26, 2009